ICRC 2001

Gamma-ray emission from the blazar Mkn 421 in 2000 and 2001, as observed by the CAT Cherenkov Imaging Telescope above 250 GeV

B. Khélifi for the CAT Collaboration

Physique Corpusculaire et Cosmologie, Collège de France et Université Paris VII, France (IN2P3/CNRS)

Abstract. The γ-ray emission above 250 GeV from the BL Lac object Markarian 421 has been observed by the CAT Cherenkov Imaging Telescope since December, 1996. In 2000 and 2001, the source showed an activity much higher than during the previous 3 years. Results on the source variability and on its energy spectrum obtained from observations during years 2000 and 2001 are reported.

1 Introduction

Markarian 421 (Mkn 421) is, along with Markarian 501 (Mkn 501), one of the two BL Lac objects confirmed as sources of TeV γ-rays (Punch *et al.* (1992), Petry *et al.* (1996), Krennrich *et al.* (1997), Holder *et al.* (2000), Piron *et al.* (2001)). It has been also one of the most studied blazars and the target of several multi-wavelength observation campaigns from the radio band to the γ-ray range. Both Mkn 421 and Mkn 501 occasionally produce spectacular flares in the very high energy (VHE) range. The CAT (Cherenkov Array at Themis) imaging telescope has been monitoring this source since December, 1996. During the 2000 and 2001 observation campaigns with CAT, Mkn 421 showed a much higher activity than during the preceding years. This paper summarizes the results on light curves and on energy spectra obtained from CAT observations during this period.

2 Experimental setup and data analysis

The CAT instrument (Barrau *et al.*, 1998) is an imaging Cherenkov telescope (17.8 m^2 reflector area) located on the site of the former solar plant Thémis in the French Pyrénées (2° East, 42° North, altitude 1650 m above sea level). Very high definition imaging of cosmic-ray showers is achieved by means of a camera using 546 phototubes with 0.12° angular diameter in a 3.1° field of view, surrounded by larger phototubes in two guard rings extending the field of view to

Correspondence to: B. Khélifi (khelifi@in2p3.fr)

4.8°. Due to the fast trigger electronics located in the camera, the detection threshold (defined as the energy at which the differential γ-ray rate is maximum at the trigger level for a Crab-like source) is as low as 250 GeV at Zenith. The very high definition of shower images allows an efficient rejection of proton and nucleus-induced events by means of an accurate analysis based on the comparison of individual images with theoretical mean γ-ray images (Le Bohec *et al.*, 1998). A χ^2 fit to a mean light distribution predicted from electromagnetic showers simultaneously provides the likelihood level of a γ-ray origin and, if this hypothesis is correct, a measurement of the γ-ray energy with an accuracy (r.m.s.) of 22%. Furthermore, due to the strong anisotropy of Cherenkov light, the longitudinal light profile of the image allows the source position to be fitted for each shower with an accuracy of the order of the pixel size, allowing a bright source to be localized with an accuracy better than 1'.

The analysis, which allows the extraction of the γ-ray signal, is described in detail in Piron *et al.* (2001). After a first cut requiring that the total charge in the image be greater than 30 photo-electrons (p.e.), the discrimination between γ and hadron-induced showers is based on the shape and the orientation of the images. The shape cut is achieved by requiring a χ^2 probability greater than 0.35. In addition, since γ-ray images are expected to point towards the source angular position in the focal plane whereas cosmic-ray directions are isotropic, a second cut $\alpha < 6°$ is used in the case of a point-like source, where the pointing angle α is defined as the angle at the image barycentre between the actual source angular position and the source position as reconstructed by the fit. As a result, this procedure rejects 99.5% of hadronic events while keeping 40% of γ-ray events; the Crab nebula, which is generally considered as the standard candle for VHE γ-ray astronomy, is detected at a 4.5σ level in one hour. The hadronic backround surviving the preceding cuts is monitored by comparing ON and OFF-source observations at the same telescope elevation. After April 2001, in order to optimize the observation time, data have been taken with the source S shifted 0.29° away from the center O of the field of

view; showers pointing to the symmetrical position S' with respect to O have been used to monitor the background and considered as OFF-source data. Showers pointing ambiguously to S and S' have been rejected. This procedure, used for zenith angles smaller than $45°$, results in a small reduction of the effective detection area but allows a more continuous monitoring of the source.

As in all cosmic-ray experiments, the limited energy resolution is a critical parameter in the determination of a steep spectrum, since it results in a considerable event flow into higher *estimated* energy intervals. The present study is based on a forward-folding method in which *a parametrization of the spectrum* has been assumed. The detector response (effective detection area, energy resolution) being determined by detailed simulations, a maximum likelihood method has been used to directly determine the relevant spectral parameters from the distributions of estimated energies of ON and OFF-source γ-ray candidates for different bins in zenith angle. The likelihood-function expression does not rely on a straightforward "ON–OFF" subtraction as in usual spectral analyses, but on the *respective* Poissonian distributions of ON and OFF events, thus allowing possible low statistics to be treated in a rigorous manner. Furthermore, no hypothesis is required on the background (OFF) shape. The complete procedure is explained in detail in Piron *et al.* (2001). two hypotheses are successively considered for the differential γ-ray spectrum $\frac{d\phi}{dE}$: *i)* a simple power law, $\phi_0^{\mathrm{pl}} \, E_{\mathrm{TeV}}^{-\gamma^{\mathrm{pl}}}$ (hyp. $\mathcal{H}^{\mathrm{pl}}$), which is often a good approximation, at least within a restricted energy range (over one or two orders of magnitude), and *ii)* a curved shape, $\phi_0^{\mathrm{cs}} E_{\mathrm{TeV}}^{-(\gamma^{\mathrm{cs}}+\beta^{\mathrm{cs}} \log_{10} E_{\mathrm{TeV}})}$ (hyp. $\mathcal{H}^{\mathrm{cs}}$). The latter parameterization, previously used by the Whipple group for the study of Mkn 421 and Mkn 501 (Krennrich *et al.*, 1999), corresponds to a parabolic law in a $\log(\nu F(\nu))$ *vs.* $\log(\nu)$ representation, where $\nu F(\nu) \equiv E^2 \frac{d\phi}{dE}$ and $E = h\nu$.

The relevance of $\mathcal{H}^{\mathrm{pl}}$ with respect to $\mathcal{H}^{\mathrm{cs}}$ is estimated from the likelihood ratio of the two hypotheses, which is defined as $\lambda = 2 \log\left(\frac{\mathcal{L}^{\mathrm{cs}}}{\mathcal{L}^{\mathrm{pl}}}\right)$: it behaves (asymptotically) like a χ^2 with one degree of freedom and permits the search for possible spectral curvature. For each data sample, the spectral law finally retained is given by the most relevant parameterization of the differential spectrum. In the following, we chose to represent each spectrum as a function of the *true* photon energy by an area corresponding to the 68% confidence level contour given by the likelihood method.

3 Results

3.1 Data sample and light curves

The complete data sample of observations consists of observations taken between December, 1999 and the end of April, 2001. We selected this sample based on clear weather conditions and stable detector operation. This selection leaves a
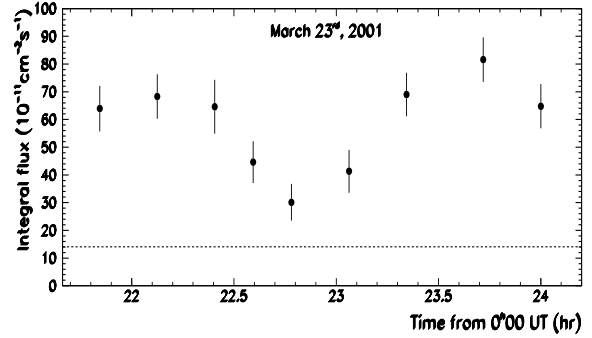

Fig. 2. Mkn 421 integral flux above 250 GeV during the night of March 23$^{\mathrm{rd}}$, 2001 (MJD 51991/92). Each point indicates for a $\sim$15 min observation, the dashed line shows the Crab nebula level emission ($\Phi_{>250\,\mathrm{GeV}} = 14.10 \pm 0.35 \times 10^{-11}$ cm^{-2} s^{-1}). The χ^2 per d.o.f corresponding to a constant flux is 5.64.

total of 46.7 hours of on-source (ON) data and 69.1 hours on control (OFF) regions, all taken within a zenith angle range extending from close to the Zenith to $40°$. The number of γ-rays is obtained by "ON-OFF" subtraction, and we suppose a spectral shape for the calculation of the effective area of the detector per zenithal angle band. The light curves of the two periods of observation are presented in Fig. 1. We used a power-law spectrum with a differential index of -2.9, which is the mean index of the two periods. This index results from the fitting procedure described in Sect. 2 and detailed below. The integral fluxes are estimated above 250 GeV for all data. A full description of the method can be found in Piron *et al.* (2001).

Figure 1 shows that the mean flux of Mkn 421 is significantly higher during the years 2000–01 ($\Phi_{>250\,\mathrm{GeV}} = 20.4 \pm 0.6 \times 10^{-11}$ cm^{-2} s^{-1}) than during 1999–2000 ($\Phi_{>250\,\mathrm{GeV}} = 9.0 \pm 0.5 \times 10^{-11}$ cm^{-2} s^{-1}). The latter period is marked by two episodes of strong activity during the months of February and April 2001. Their level of activity is higher than the flare state of January and February 2000. The night of March 23/24, 2001, is remarkable for the strong activity of the source: $\Phi_{>250\,\mathrm{GeV}} = 67.3 \pm 2.6 \times 10^{-11}$ cm^{-2} s^{-1}. Nevertheless, the sampling of the 2000–01 period is poor due to bad weather conditions in the Pyrénées.

The intra-night variability of March 23$^{\mathrm{rd}}$, 2001 can be seen in Fig. 2. The high flux level of the source and the stable weather have allowed us to use 15 min timing samples. A curved spectral hypothesis is used for this light curve; its parameters are $\gamma^{\mathrm{cs}} = 2.80$ and $\beta^{\mathrm{cs}} = 0.81$ (see the next section). The flux intensity of Mkn 421 varies over a range of $\sim$4.0 times the flux of Crab nebula (which is $\Phi^{\mathrm{CN}} = 14.10 \pm 0.35 \times 10^{-11}$ cm^{-2} s^{-1} above 250 GeV, see Piron (2000)) over 1 hour. The maximum measured flux rises to $\sim$6.1Φ^{CN} ($\Phi_{>250\,\mathrm{GeV}} = 86.4 \pm 8.4 \times 10^{-11}$ cm^{-2} s^{-1}).
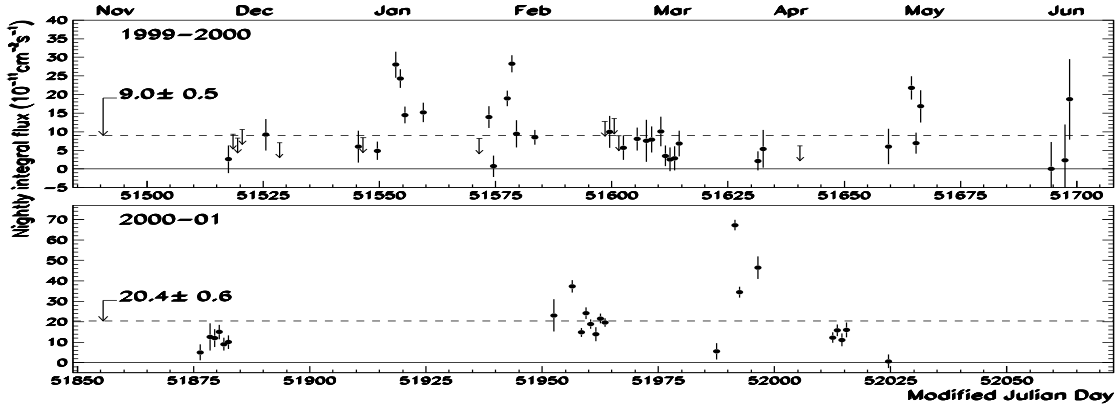
Fig. 1. Mkn 421 nightly-averaged integral flux above 250 GeV between December, 1999 and May, 2001. The γ-ray effective area has been weighted using a differential index of -2.9, in order to estimate the integral flux for observations far from the Zenith (see (Piron *et al.*, 2001)). Arrows stand for $2\,\sigma$ upper-limits when no signal was recorded, and dashed line shows the mean flux for each observation year.
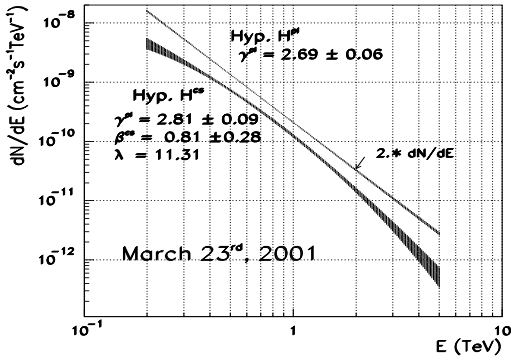

Fig. 3. Mkn 421 time-averaged spectra between 0.3 and 5.0 TeV in March 23rd, 2001. The curve labelled *Hyp. H^{pl}* uses a power-law shape, and the one refereced by *Hyp. H^{cs}* uses a curved shape. The differential flux of the power-law hypothesis is multiplied by a factor of two for the clarity of the picture.

3.2 Energy spectra in 2000 and 2001

The data sample used to estimate the time-averaged spectra is chosen using more stringent criteria in terms of detector stability than those used for the light curves. The extraction of the spectral shape is described in Sect. 2. The data used in the 2000 and 2001 periods covers a range out to a zenith angle of $40°$ and to $20°$ for the March 23rd, 2001 data.

The night of March 23rd, 2001, contains the bigger flare state of Mkn 421 from our data-base. The maximum measured integrated flux rises to $\sim 6.1\ \Phi^{\mathrm{CN}}$ (see above). The spectrum during this night is presented in Fig. 3.

The likelihood ratio value of our tested hypotheses is equal

to 11.3, which significantly shows a curved spectrum (the associated probability is 7.7×10^{-4}). We adopt the following characterisation for the night of March 23rd, 2001:

$$\frac{\mathrm{d}\phi}{\mathrm{d}E} = (12.44 \pm 0.81^{\mathrm{stat}} \pm 2.49^{\mathrm{syst}})10^{-11}\ \mathrm{cm}^{-2}\ \mathrm{s}^{-1}\ \mathrm{TeV}^{-1}$$

$$\times E_{\mathrm{TeV}}^{-2.80 \pm 0.09^{\mathrm{stat}} \pm 0.06^{\mathrm{syst}} - (0.81 \pm 0.27^{\mathrm{stat}} \pm 0.03^{\mathrm{syst}}) \log_{10} E_{\mathrm{TeV}}}.$$

The systematic errors quoted here are derived using detailed simulations.

Fig. 4 shows the spectrum for the 1999–2000 and 2000–01 periods; on the left hand plot we suppose a power-law shape, and on the right hand plot a curved shape. The fitted parameters are summarized in Table 1. These spectral shapes are compatible with a power-law, although there is some evidence for curvature. The likelihood ratio values are 4.90 for 2000 (corresponding to a chance probability of 0.027), and 5.51 for 2001 (a chance probability of 0.019). We can conclude that the time-averaged spectra for the 2 years are consistent in spectral slope to less than 2σ on statistical errors. Thus we retain the following characterisation for the 2001 period:

$$\frac{\mathrm{d}\phi}{\mathrm{d}E} = (3.47 \pm 0.16^{\mathrm{stat}} \pm 0.69^{\mathrm{syst}})10^{-11}\ \mathrm{cm}^{-2}\ \mathrm{s}^{-1}\ \mathrm{TeV}^{-1}$$

$$\times E_{\mathrm{TeV}}^{-2.87 \pm 0.05^{\mathrm{stat}} \pm 0.06^{\mathrm{syst}} - (0.38 \pm 0.17^{\mathrm{stat}} \pm 0.03^{\mathrm{syst}}) \log_{10} E_{\mathrm{TeV}}}.$$
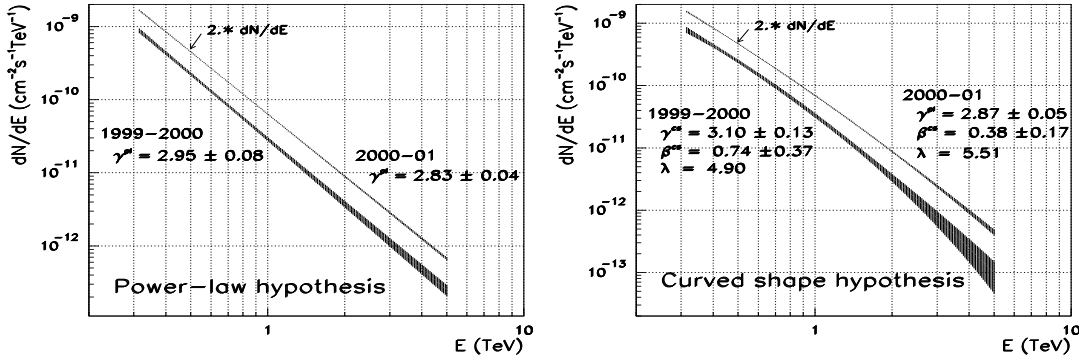
Fig. 4. Mkn 421 time-averaged spectra between 0.3 and 5.0 TeV in 1999–2000 and 2000–01. The areas show the 68% confidence level contour given by the likelihood method. On the left hand, we suppose a power-law hypothesis, and on the right hand a curved shape hypothesis. The differential flux of 2000–01 are multiplied by a factor of 2 for the clarity of the picture.

Period	$\Delta\widetilde{E_\gamma}$ (TeV)	S_γ	$\phi_0^{\rm pl}$	$\gamma^{\rm pl}$	$E_{\rm d}$	$\phi_0^{\rm cs}$	$\gamma^{\rm cs}$	$\beta^{\rm cs}$	$E_0^{\rm cs}$	$\gamma_0^{\rm cs}$	λ
1998−99	0.3−5.0	735±57	2.29±0.20	2.88±0.12	0.69	2.51±0.32	2.94±0.15	0.40±0.48	0.73	2.88±0.14	0.75
1999−2000	0.3−5.0	1424±71	2.90±0.18	2.95±0.08	0.63	3.34±0.28	3.10±0.13	0.74±0.37	0.61	2.94±0.10	4.90
2000−01	0.3−5.0	5612±157	3.18±0.10	2.83±0.04	0.68	3.47±0.16	2.87±0.05	0.38±0.17	0.73	2.82±0.05	5.51
23/03/2001	0.3−5.0	1320±50	10.50±0.49	2.68±0.06	0.64	12.44±0.81	2.80±0.09	0.81±0.27	0.67	2.67±0.08	11.3

Table 1. Characteristics of the Mkn 421 spectra obtained in this paper. For each spectrum we indicate the observation period, the total energy band used in the likelihood method, $\Delta\widetilde{E_\gamma}$, the total observed number of γ-ray events, S_γ, the spectral parameters obtained in the $\mathcal{H}^{\rm pl}$ and $\mathcal{H}^{\rm cs}$ hypotheses, and the likelihood ratio λ. We also quote the decorrelation energy in the $\mathcal{H}^{\rm pl}$ hypothesis, $E_{\rm d}$, the energy $E_0^{\rm cs}$ at which the energy-dependent exponent $\gamma_l^{\rm cs}(E_{\rm TeV})=\gamma^{\rm cs}+\beta^{\rm cs}\log_{10} E_{\rm TeV}$ has a minimal error in the $\mathcal{H}^{\rm cs}$ hypothesis (see Piron *et al.* (2001)), and the corresponding value $\gamma_0^{\rm cs} \equiv \gamma_l^{\rm cs}(E_0^{\rm cs})$. The energies are given in TeV, and the flux constants in units of 10^{-11} cm^{-2} s^{-1} TeV^{-1}.

4 Discussion and conclusions

During the past year Mkn 421 had the highest activity since 1996 as seen by CAT. The period 2000–01 has a mean integrated flux of $\Phi_{>250\,{\rm GeV}}=20.4 \pm 0.6 \times 10^{-11}$ cm^{-2} s^{-1} and the source flux rises to $\sim$6.1 flux level of Crab nebula ($\Phi^{\rm CN}$) during the night of March 23$^{\rm rd}$, 2001. In this night, the source flux decreased and then increased by a factor of 3-4 $\Phi^{\rm CN}$ over a timescale of 1 hour. The 2001 time-averaged spectrum of Mkn 421 is well parametrised by a curve shape, as is the spectrum of the night of 23$^{\rm rd}$ for which the curvature is clearly observed.

If we compare the spectrum of Mkn 421 between different years which have different activities (see Table 1), we note that no apparent curvature is visible for a low flux level (e.g., in 1998), while for the years 2000 and 2001 a curvature appears weakly, then for a high flux activity (e.g., March 23$^{\rm rd}$, 2001) a significant curvature becomes visible. And we can note that, for an energy range below $\sim$2 TeV, the spectral shape for the March 23$^{\rm rd}$, 2001 is flatter than the shape in the previous years. Thus, in the framework of blazar models exhibiting a spectral energy distribution with double peaks (a synchrotron component at low energy and an Inverse Compton peak in the MeV/GeV range), the energy value of the high energy peak maximum seems to become higher when the measured flux activity rises. This maximum peak energy comes closer to our detector's energy range and a spectral variability appears. At the same time, simultaneous BeppoSAX observations in March 2001 have shown a hardening of spectrum in the X-ray range (Fossati *et al.*, 2001) as compared to previous years. It is then most likely that the spectral characteristics seen for March 23$^{\rm rd}$, 2001 are due to a more efficient acceleration process or/and to an enhancement of the injected electron population.

References

Barrau, A.,*et al.* 1998, NIM A416, 278

Fossati, G.,*et al.* 1998, MNRAS 299, 433

Fossati, G.,*et al.* 2001, Gamma 2001 Conf., Baltimore

Holder, J.,*et al.* 2000, High Energy Gamma-Ray Astronomy, Eds. F.A. Aharonian and H.J. Voelk, AIP Conf. Proc. 558, 635

Krennrich, F.,*et al.* 1997, ApJ 481, 758

Krennrich, F.,*et al.* 1999, ApJ 511, 149

Le Bohec, S.,*et al.* 1998, NIM A416, 425

Petry, D.,*et al.* 1996, A&A 311, L13

Piron, F.,*et al.* 2001, A&A to be published

Piron, F. 2000, Ph.D. Thesis, University of Orsay-Paris XI (http://lpnhp2.in2p3.fr/homecat/publi.html)

Punch, M.,*et al.* 1992, Nature 358, 477